# Supplementary Information

# Spike sorting using non-volatile metal-oxide memristors

Isha Gupta[a,*], Alexantrou Serb[a], Ali Khiat[a], Maria Trapatseli, Themistoklis Prodromakis[a].

[a]Electronic Materials and Devices Research Group, Zepler Institute for Photonics and Nanoelectronics, University of Southampton, SO17 1BJ, Southampton, UK. Corresponding Author*: Isha Gupta (Email: I.Gupta@soton.ac.uk)

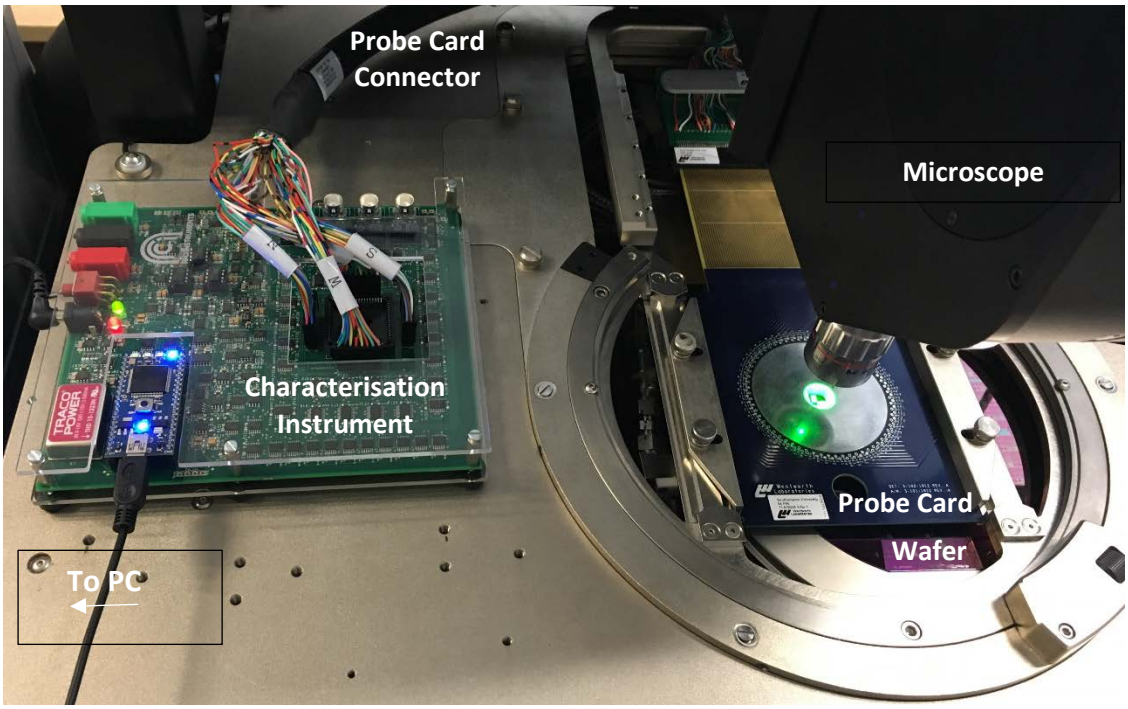


**Supplementary Figure 1** Experimental setup for the spike sorting experiments. The devices were electrically characterised using a custom-made hardware characterisation instrument[1]. The instrument can be used to characterise devices both in-package and directly on-wafer via probe card. For the demonstrated experiments, both packaged and on-wafer devices were used[2,3].

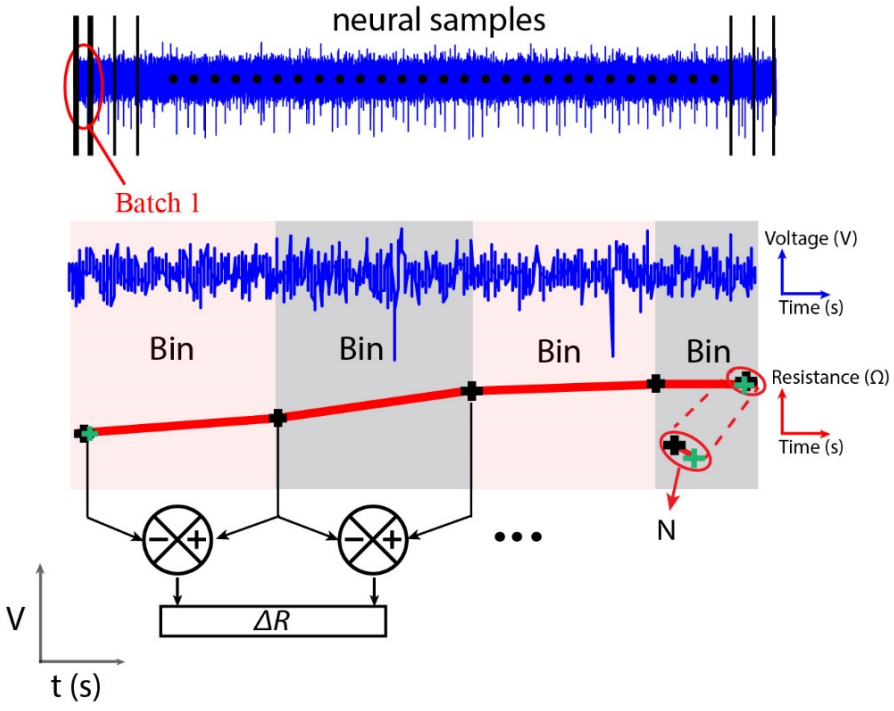


(b)

**Supplementary Figure 2**[3,4] Signal-processing strategy used for the memristor-based spike sorter[3]. The neural signal is fed to the devices in batches. The batches are further divided in smaller bins and the resistive state of the device is read after each bin. Batch and bin sizes are flexible and can be set by the user to suit experimental needs[5]. Importantly, after each batch, the neural recording is paused and one additional resistive state measurement is taken in order to estimate noise levels (green cross in (b)). Therefore, during post-processing, consecutive resistive state readings are used to estimate the changes in resistive state of the device and the readings at the end of each batch are used to estimate the noise. For spike sorting, the changes in resistive state registered in each bin are plotted as a function of the initial resistive state for each bin.

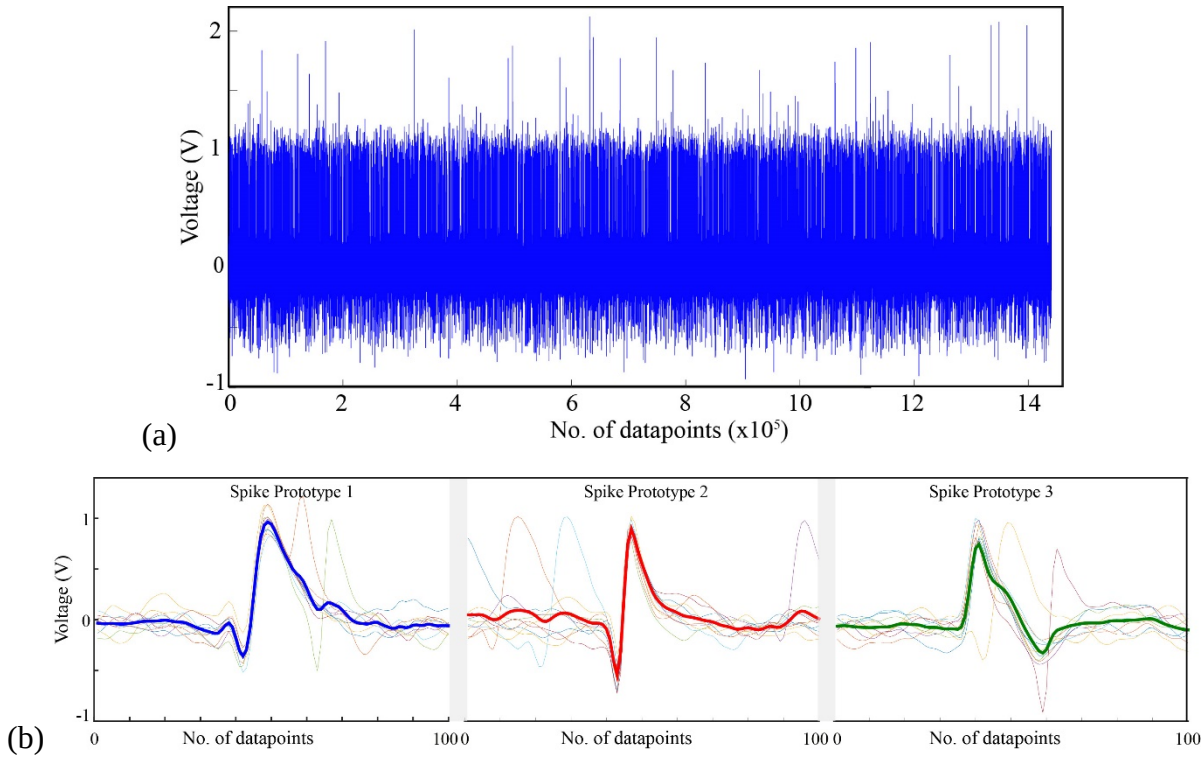


**Supplementary Figure 3** (a) Raw neural recording data used for the experiments. The data is publicly available from University of Leicester (http://www2.le.ac.uk/centres/csn/software, Dataset 2[6]. The neural recording contains three distinct single-unit spike waveforms superposed on background noise. Detailed description on how this neural recording data was synthesised is presented in the reference[6]. (b) For our experiments, we randomly extracted ten different instances of each spike prototype as illustrated in the three insets. The spike timings of the instances are documented in Supplementary Table 1. Each instance of every spike waveform contains 100 data points i.e. 19 points before and 80 points after the spike registration timestamp. Thick blue, green and red traces show the averages of ten different instances of each spike waveform. The maximum and minimum voltage values in each average spike prototype are further presented in Supplementary Table 2.

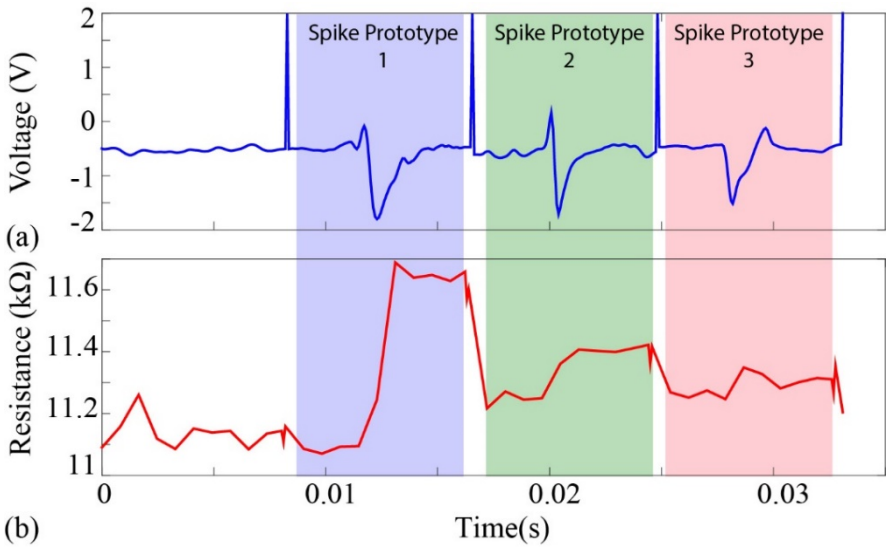


**Supplementary Figure 4** (a) Pre-processed recording used for Figure 1(b-g) in the main manuscript. The gain and offset used for the recording was -1.31 and -0.63V. Reset pulses of +2V were used to maintain the device functionality within the operational resistive state region. (b) Resistive state changes for the device in response to the recording in (a) over time. Blue, green and red shadings correspond to the three distinct average prototypes 1, 2 and 3 respectively.

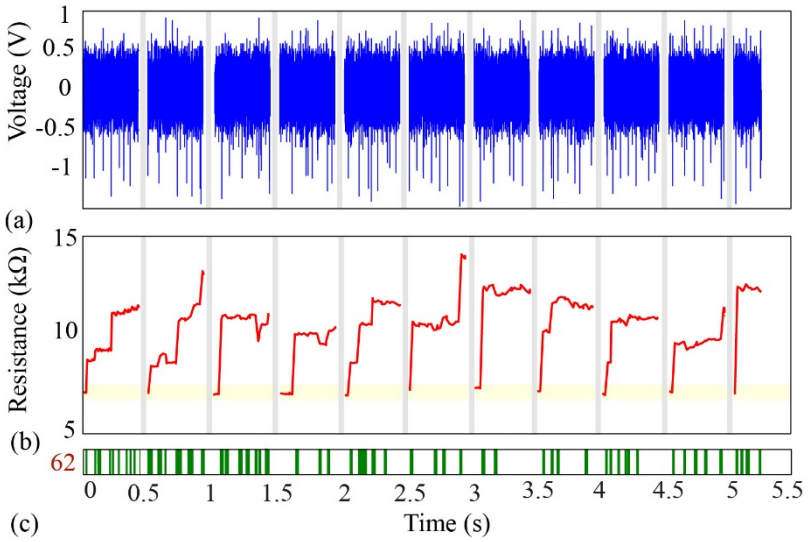


**Supplementary Figure 5**[4] Frequent resetting of the memristive device (non-volatile regime[4]). Continuous operation of the memristive device in the non-volatile region for input signals dominated by peaks of a single polarity results in saturation of the resistive state of the device. As a mitigation measure, reset pulses shown in grey band are interspersed with the neural signal. (a), (b) Resistive state response of the device-under-test in response to the sub-neural recordings. After every sub-neural recording the device is reset to its intital resistive state (yellow bands) using a pulse of positive polarity of 100 µs. The intital resistive state of the device is in the region of 6-8 kΩ and the operation of the device is in the region of 6 kΩ (low

resistive state) to 15 kΩ (high resistive state). (c) Raster of detected spikes. Total spike count: 62.

| S.No. | Resistive State Reads (RSR's - Ω) | Batch 1 | RSR's | Batch 2 | RSR's | Batch 3 | RSR's | Batch 4 |
|---|---|---|---|---|---|---|---|---|
| | Background/Resets | | Spike III | | Spike II | | Spike I | |
| 1. | 11757.99 | B1 | 11782.02 | B13 | 11898.06 | B25 | 12311.09 | B37 |
| 2. | 11828.519 | B2 | 11763.65 | B14 | 11886.4 | B26 | 12232.41 | B38 |
| 3. | 11790.73 | B3 | 11757.92 | B15 | 11809.14 | B27 | 12235.02 | B39 |
| 4. | 11699.33 | B4 | 11760.06 | B16 | 11983.17 | B28 | 12241.67 | B40 |
| 5. | 11790.91 | B5 | 11706.08 | B17 | 11855.17 | B29 | 12267.59 | B41 |
| 6. | 11790.03 | B6 | 11894.95 | B18 | 12191.47 | B30 | 12653.33 | B42 |
| 7. | 11783.03 | B7 | 11899.9 | B19 | 12244.21 | B31 | 12843.73 | B43 |
| 8. | 11697.71 | B8 | 11924.52 | B20 | 12283.07 | B32 | 12776.11 | B44 |
| 9. | 11755.08 | B9 | 11834.5 | B21 | 12238.37 | B33 | 12796.08 | B45 |
| 10. | 11766.31 | B10 | 11841.8 | B22 | 12179.92 | B34 | 12816.69 | B46 |
| 11. | 11739.83 | B11 | 11889.99 | B23 | 12279.27 | B35 | 12813.46 | B47 |
| 12. | 11784.81 | B12 | 11855.77 | B24 | 12202.14 | B36 | 12834.55 | B48 |
| Fractional Changes in Resistive state – ignoring data point at S. No. = 1 | | | | | | | | |
| S.No. (10-2) | -0.52 | | 0.66 | | 2.47 | | 4.77 | |
| S.No. (11-2) | -0.75 | | 1.07 | | 3.30 | | 4.75 | |
| S.No. (12-2) | -0.37 | | 0.78 | | 2.65 | | 4.92 | |
| Averages | -0.55 | | 0.84 | | 2.81 | | 4.82 | |
| Fractional Change in Resistive state – including data point at S. No. = 1 | | | | | | | | |
| S.No. (10-1) | 0.07 | | 0.50 | | 2.37 | | 4.10 | |
| S.No. (11-1) | -0.15 | | 0.92 | | 3.20 | | 4.08 | |
| S.No. (12-1) | 0.23 | | 0.62 | | 2.55 | | 4.25 | |
| Average | 0.048 | | 0.68 | | 2.70 | | 4.14 | |

**Supplementary Table 1** Raw resistive state measurements taken during the first spike triplet shown in Figure 4 in the main text. Each resistive state read-out is indexed with a unique identifier ('B1, B2, …'). Each batch contains 100 input data points and each bin contains 10 input data points. This means that resistive state measurements were taken at the beginning of each batch of size 100 and then after every bin of size 10. One final measurement was taken at the end of batch whilst the neural feed was paused (noise estimation – see Figure 2). **Important:** (a) For estimating the fractional change in resistive states for each spike prototype in the spike triplet, resistive states highlighted in yellow and pink were used as the initial and final resistive states respectively. (b) For estimating fractional changes in resistive states due to background noise/resets, resistive states indicated in yellow and peach colours (S.No. 11/12) were used as the initial and final resistive states respectively. The averages of these values were plotted in Figure 3(b,d) as a function of the initial resistive state.

| | RSR (% change) | Initial RS (Ω) | RSR (% change) | Initial RS (Ω) | RSR (% change) | Initial RS (Ω) | RSR (% change) | Initial RS (Ω) |
|---|---|---|---|---|---|---|---|---|
| Spike Triplet (Order fed) | Background Resets | | Spike III | | Spike II | | Spike I | |
| Spike Triplet 1 (3,2,1) | -0.009 | 12392.02 | 3.13 | 12400.28 | 6.083 | 13111.9 | 1.012 | 14022.04 |
| Spike Triplet 2 (3,1,2) | -0.35 | 16769.94 | 7.61 | 13351.12 | 1.10 | 16514.83 | 14.245 | 14387.25 |
| Spike Triplet 3 (1,3,2) | 0.331 | 16012.95 | 0.492 | 15939.68 | 1.92 | 15721.62 | 10.3 | 14407.54 |
| Spike Triplet 4 (2,3,1) | 0.52 | 16265.24 | 1.40 | 15812.35 | 7.752 | 14267.21 | 0.72 | 16012.79 |
| Spike Triplet 5 (1,3,2) | -0.61 | 16277.72 | 0.13 | 16337.895 | 0.663 | 16246.95 | 14.57 | 0.45586 |
| Spike Triplet 6 (2,3,1) | -0.091 | 16451.23 | -0.41 | 16518.9 | 0.455 | 14365.22 | 12.22 | 14525.54 |
| Spike Triplet 8 (1,2,3) | -0.47 | 15875.08 | -0.45 | 15775.74 | -0.29 | 15827.51 | 8.88 | 14395.29 |
| Spike Triplet 9 (2,3,1) | -0.025 | 15591.67 | -1.38 | 15698.12 | 7.12 | 14452.56 | 6.9 | 15719.95 |
| Spike Triplet 10 (3,1,2) | -0.052 | 17298.12 | 9.90 | 14640.5 | 0.61 | 17190.34 | 4.75 | 16335.51 |

**Supplementary Table 2:** Result summary for Figure 6. Measured resistive states and fractional changes in resistive state experienced by the memristor as a result of applying the ten spike triplets from Figure 6(a). In each row, the effects of the different spike components of each triplet are shown separately.

## REFERENCES


1. Serb, A., Berdan, R., Khiat, A., Papavassiliou, C. & Prodromakis, T. Live demonstration : A versatile , low-cost platform for testing large ReRAM cross-bar arrays . *IEEE Int. Symp. CIRCUITS Syst.* **9,** 4799 (2014).

2. Gupta, I. *et al.* A Cell Classifier for RRAM Process Development. *IEEE Trans. Circuits Syst. II Express Briefs* (2015). doi:10.1109/TCSII.2015.2415276

3. Gupta, I. *et al.* Real-time encoding and compression of neuronal spikes by metal-oxide memristors. *Nat. Commun.* **7,** 1–16 (2016).

4. Gupta, I., Serb, A., Khiat, A. & Prodromakis, T. Improving detection accuracy of memristor-based bio-signal sensing platform. *IEEE Trans. Biomed. Circuits Syst.* 1–9 (2016). doi:10.1109/TBCAS.2016.2580499

5. Gupta, I. *et al.* Real-time coding and compression of neuronal spikes by metal-oxide memristors. *Nat. Commun.* (2016). doi:10.1038/ncomms12805

6. Quiroga, R. Q., Nadasdy, Z. & Ben-Shaul, Y. Unsupervised spike detection and sorting with wavelets and superparamagnetic clustering. *Neural Comput.* **16,** 1661–1687 (2004).